Stable Silver Nanoparticles Immobilized in Mesoporous Silica

Virginie Hornebecq,*,† Markus Antonietti,† Thierry Cardinal,‡ and Mona Treguer-Delapierre‡

Max-Planck-Institute of Colloids and Interfaces, Research Campus Golm, D-14424 Potsdam, Germany, and Institut de Chimie de la Matière Condensée de Bordeaux, 87 Avenue du Dr A. Schweitzer, 33608 Pessac Cedex, France

Received November 12, 2002. Revised Manuscript Received February 25, 2003

Silver nanoparticles have been produced by γ-irradiation of silver solution in optically transparent inorganic mesoporous silica. The reduction of Ag^+ within the matrix is brought about by hydrated electrons and hydroalkyl radicals generated during the radiolysis of the 2-propanol solution. The particles formed within the silica matrix were studied by electron microscopy, nitrogen sorption measurements, and absorption spectroscopy. The particles were mostly confined and dispersed in the pores of the mesoporous hosts. Absorption spectra show that the mean Ag clusters size increases with the irradiation dose. At high dose, agglomerated large particles are formed. In contrast, at a given dose, the effect of the dose rate has been clearly demonstrated to lower the cluster size. The silver particles within the silica matrix are stable in the presence of oxygen for at least several months.

Introduction

The increase of luminescence and scattering due to surface and size quantization effects is a very promising route for the improvement of optical devices (communication, optical storage, detectors, etc.). Recently, several articles have shown the possibility of enhancing by a least 1 order of magnitude the emission efficiency of a luminescent center in the vicinity of a conducting metallic particle in a manner analogous to the surface-enhanced Raman scattering.[1−3] Depending on the size and the composition of the metallic particles, different fluorescent enhancement phenomena were observed. It has been demonstrated in low silver content phosphate glass that the presence of micrometer-size silver metallic particles can lead to broad and intense luminescence compared to pure silver phosphate glass.[4] The luminescence was evidenced to appear near the surface of the particle and is due to the coupling of Ag^+ ions with the silver particles. Recently, Dickson et al. demonstrated that an intense luminescence can be obtained after partial reduction of an silver oxide film and the formation of nanometric metallic particles on the surface.[5]

The mechanism of these metal surface luminescent enhancement effects are not truly understood. For practical applications, it is important to realize a maximum density of isolated silver particles in a confined volume so that practically all the solute is in nanometer-close proximity to a silver surface and the coupled plasmons. For that, considerable progress has to be made in controlling the distance between the metallic particle and the potentially luminescent or oscillating center and controlling the size, the geometry, and the dimensionality of this composite system.

The use of a monolithic or filmlike matrix of mesoporous silica with well-defined pore size and connectivity to nest the composite system should allow such a system to be obtained. Here, the nanometer-size particles with a narrow size distribution is ensured by the pore size, whereas control of the particles distance and particle separation is guaranteed by the pore walls. It is not new to synthesize nanoscale particles (metal or semiconductors, composites) inside the pores of particulate zeolithes or mesoporous powders.[6] For instance, it has been found that metal nanoparticles could be easily produced via an impregnation process of ionic precursors onto the porous solids followed by thermal reducing treatment.[7−9] In a similar way, a sonochemical method was used to prepare metal or metal alloy particles by exposing the solution of the ionic metal precursor in the presence of silica to ultrasound.[10] Hg, Ag, Pb, or Cu clusters in silica have been also prepared by voltametry.[11] More recently, silver particles in mesoporous silica film have also been

* To whom correspondence should be addressed. E-mail: Virginie.Hornebecq@mpikg-golm.mpg.de.
† Max-Planck-Institute of Colloids and Interfaces.
‡ Institut de Chimie de la Matière Condensée de Bordeaux.

(1) Doering, W. E.; Nie, S. *J. Phys. Chem. B* **2002**, *106*, 311, and references therein.
(2) Félix, C.; Sieber, C.; Harbich, W.; Buttet, J.; Rabin, I.; Schulze, W.; Ertl, G. *Phys. Rev. Lett* **2001**, *86*, 2992, and references therein.
(3) Peyser, L. A.; Vinson, A. E.; Bartko, A. P.; Dickson, R. M. *Science* **2002**, *291*, 103.
(4) Belharouak, I.; Weill, F.; Parent, C.; Le Flem, G.; Moine, B. *J. Non-Cryst. Solids* **2001**, *293−295*, 649.
(5) Lee, T. H.; Gonzalez, J. I.; Dickson, R. *Proc. Natl. Acad. Sci.* **2002**, *99*, 10272.
(6) Zhang, W. H.; Shi, J. L.; Wang, L. Z.; Yan, D. G. *Chem. Mater.* **2000**, *12*, 1408, and references therein. Sheppard, D. S.; Maschmeyer, T.; Johnson, B.; Thomas, J.; Sankar, G.; Ozkaya, D.; Zhou, W.; Oldroyd, R.; Bell, R. *Angew. Chem., Int. Ed. Engl.* **1997**, *36*, 2242, and references therein.
(7) Cai, W.; Zhang, L. *J. Phys.: Condens. Matter* **1997**, *9*, 7257. Cai, W.; Zhang, Y.; Jia, J.; Zhang, L. *Appl. Phys. Lett.* **1998**, *73*, 19.
(8) Cai, W.; Hofmeister, H.; Rainer, T. *Physica E* **2001**, *11*, 339.
(9) Plyuto, Y.; Berquier, J.-M.; Jacquiod, C.; Ricolleau, C. *Chem. Commun.* **1999**, 1653.
(10) Cai, W.; Hofmeister, H.; Rainer, T.; Chen, W. *J. Nanopart. Res.* **2001**, *3*, 443.

10.1021/cm021353v CCC: $25.00
Published on Web 04/24/2003

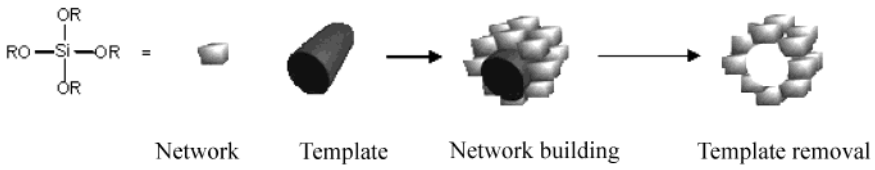

Figure 1. Schematic representation of the nanocasting concept.

synthesized using the pulsed laser deposition (PLD) technique.[12] Such materials can also be made by one-step procedures using special metal precursors that act simultaneously as templates for the formation of porous silicas.[13,14]

In the present study, we focus on the preparation of silver nanoparticles nested into mesoporous silica. Silver was chosen because of the newly discovered luminescence of Ag^+/Ag nanoparticles, and the favorable positioning of its plasmon band in the blue visible, which allows use of standard lasers for nanoparticle-enhanced optical experiments.[3,5] The silica framework was chosen because of its transparence. For a better understanding of the silver nanoparticles formation and their resulting physicochemical properties, the particles were produced by the radiation-induced reduction method.[15] The ionizing radiation penetrates homogeneously within the solid and ensures a homogeneous initial distribution of reducing radiolytic radicals formed by ionization and excitation of the solvent. The metallic particles are then produced homogeneously in situ within the silica framework at room temperature. Furthermore, the radiation-induced reduction method allows a control of the reducing conditions, thus of the amount of ions simultaneously reduced to form clusters of different sizes.

By combining nitrogen sorption measurements, electronic microscopy, and optical absorption methods, the silver nanoparticle formation within the silica matrix is investigated. The influence of the reduction rate on the size and the distribution of size of the particles is described. We present here the results obtained for silver but the radiation-induced reduction technique can be extended to other metallic species.

Experimental Section

Preparation of Mesoporous Silica. Mesoporous silica was prepared according to the nanocasting concept developed recently by Goltner and co-workers.[16] In this synthesis, the amphiphilic lyotropic phase structure in water—directly connected to the choice of the template—is fixed by the sol−gel formation of silica in the hydrophilic domains of the template. It results in a 1:1 replica, explaining the term nanocasting (Figure 1). Several types of templates can be used to prepare mesoporous silicas presenting different pore size and morphology: supramolecular aggregates of molecules, nonionic surfactants, block copolymers, and so forth.[17]

The synthesis of the SiO_2 network is based on two reaction steps—the hydrolysis of the ortho esters of silicic acid $Si(OR)_4$ and the polycondensation of the silicic acid—and thus two reactions rates must be taken into account. The rate of the hydrolysis is mainly governed by the nature of the R group of the ortho esters. Usually, TEOS ($R=C_2H_5$) or TMOS ($R=CH_3$) are used for two main reasons: (i) Si−O−R bond breaking is very controllable and (ii) the released solvents (ethanol or methanol) can be removed by evacuation. The condensation rate can be adjusted by the pH value of the medium.

Two different types of sample were synthesized using different templates to obtain uniform mesoporous silicas with interconnected wormlike pore morphology but different pore size: a nonionic *n*-alkyl-poly(ethylene oxide) surfactant (BRIJ78 or $C_{18}E_{20}$)[18] and a polystyrene-*b*-poly(ethylene oxide) block copolymer (SE1010) with 1000/1000 molar mass for each block.[19] In this synthesis 3 g of block copolymers are dissolved in 6 g of TMOS, and then 3 g of HCl is added. All chemicals used were of highest purity grade.

After homogenization, the evolving methanol is removed in a vacuum and the resulting gels are aged for 24 h at 60 °C. Then, the templates are removed via calcinations performed at 750 °C for 12 h in a tubular oven under a stream of oxygen. According to TEM and sorption measurements, the final pore size for BRIJ78 and SE1010 are estimated to be 2 and 4 nm, respectively, and the resulting silicas are named Sil2 and Sil4.

Preparation of Silver−Silica Sample. Both silica hosts (Sil2 and Sil4) were impregnated in a solution containing Ag_2SO_4 (10 mM (Aldrich)) in the dark to prevent photochemical decomposition: 200 mg of calcinated silica (monolithic pieces) were immersed in 5 mL of silver sulfate solution and allowed to equilibrate for 1 week. After filtering, the silica was washed to remove any excess of Ag^+ from the surface. The silica sample was then added to an aqueous solution of 2-propanol (0.2 M) where propanol captures the oxidative radicals induced by ionizing irradiation. The pH value was kept at 7 to favor the adsorption of Ag^+ in the silica matrix and also to avoid undesirable hydrolysis or precipitation reactions. Before irradiation, the sample, consisting of solid silica immerged in Ag^+ solution, was purged with argon to eliminate oxygen. Irradiation was performed on those samples with a γ-source ^{137}Cs of 3000 Ci and of a mean dose rate of 2.7 $kGy \cdot h^{-1}$. Other experiments were performed with a 20-kW and 10-MeV accelerator delivering trains of 15-μs pulses through a scanning beam (1−10 Hz) at a mean dose rate of 7 $MGy \cdot h^{-1}$. The primary effects of the interaction of high-energy radiation (γ, X-ray, particle beam, etc.) with a solution of metal ions are the excitation and the ionization of the solvent. Fast subsequent processes, dissociation of excited states, ion−molecule reaction, and radical−radical recombination lead rapidly to molecular and radical species able to react with the metal ions. In aqueous solutions, hydrated electrons, hydroxyl radicals, and hydrogen are produced:[20]

$$H_2O \xrightarrow{\gamma} e_s^-,\ OH^\bullet,\ H^\bullet,\ H_2,\ H_2O_2 \qquad (1)$$

$H^\bullet$ radicals and solvated electrons are strong reducing agents able to reduce metal ions to metal atoms. Reverse oxidation

(11) Bond, A. M.; Miao, W.; Smith, T. D.; Jamis, J. *Anal. Chim. Acta* **1999**, *396*, 203.
(12) Renard, C.; Ricolleau, C.; Fort, E.; Besson, S.; Gacoin, T.; Boilot, J.-P. *Appl. Phys. Lett.* **2002**, *80*, 300.
(13) Bronstein, L. M.; Polarz, S.; Smarsly, B.; Antonietti, M. *Adv. Mater.* **2001**, *13*, 1333.
(14) Han, B.-H.; Polarz, S.; Antonietti, M. *Chem. Mater.* **2001**, *13*, 3915.
(15) Khatouri, J.; Mostafavi, M.; Amblard, J.; Belloni, J. *Chem. Phys. Lett.* **1992**, *191*, 351.
(16) Göltner, C. G.; Antonietti, M. *Adv. Mater.* **1997**, *9*, 431. Antonietti, M.; Polarz, S. *Chem. Commun.* **2002**, 2593.
(17) Soler-Illia, G. J. A. A.; Sanchez, C.; Lebeau, B.; Patarin, J. *Chem. Rev.* **2002**, *102*, 4093.
(18) Smarsly, B.; Polarz, S.; Antonietti, M. *J. Phys. Chem. B* **2001**, *105*, 10473.
(19) Göltner, C. G.; Henke, S.; Weissenberger, M. C.; Antonietti, M. *Angew. Chem., Int. Ed.* **1998**, *37*, 613.
(20) Ferradini, C.; Pucheault, J. *Biologie de l'action des Rayonnements ionisants*; Masson: Paris, 1983; p 25.

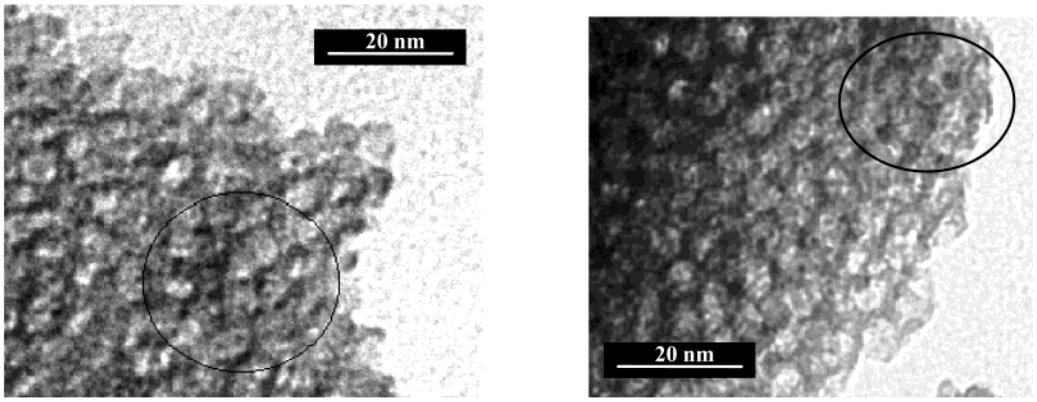

Figure 2. TEM pictures of silica−silver composite materials (Sil4) obtained at different dose rate: 7 MGy·h^{-1} (a) and 2.7 kGy·h^{-1} (b); dose = 5 kGy.

by radicals is avoided by the presence of propanol-2. The alcohol reacts with the $OH^{\bullet}$ and $H^{\bullet}$ radicals to yield 1-hydroxyethylmethyl radicals that also could efficiently reduce the metal ions when adsorbed on clusters:

$$(CH_3)_2CHOH + OH^{\bullet}\,(H^{\bullet}) \rightarrow (CH_3)_2C^{\bullet}OH + H_2O\,(H_2) \quad (2)$$

$$e_s^- + M^+ \rightarrow M^0 \quad (3)$$

$$(CH_3)_2C^{\bullet}OH + M^+ \rightarrow M^0 + (CH_3)_2CO + H^+ \quad (4)$$

The metal atoms aggregate with excess ions and other atoms to clusters of increasing nuclearity.

After the irradiation, the silica was carefully washed to remove the large particles from the surface and was then dried up to 90 °C.

The samples were characterized by nitrogen sorption analysis with a Micrometrics Gemini instrument. The samples for the sorption measurements were dried under vacuum at 373 K for 24 h. By this technique, information on the mesopore size and the specific surface area are accessible. Transmission electron microscopy (TEM) was performed to investigate the nanostructure. TEM images were acquired on a Zeiss EM 912Ω operating at an acceleration voltage of 120 kV. Samples were ground in a ball-mill and suspended in acetone. One droplet of the suspension was applied to a 400-mesh carbon-coated grid and left to dry in air. UV−vis diffusing reference spectra on powder were measured with a CARY 2415 instrument using polytetrafluoroethylene as a reference. All the spectra reported are obtained by subtraction of the parent silica spectrum from the silver−silica ones.

Results and Discussion

Addition of an aqueous solution of silver ions to solid silica results in equilibrium between the free silver ions in solution and the silver ions adsorbed in the pores of the silica:

$$SiO + Ag^+ \leftrightarrow [SiO{-}Ag^+] \quad (5)$$

The silver ions can interact with the Si−OH groups on the internal pore surfaces of the silica framework. An equilibrium constant $K = [SiO{-}Ag^+]/[SiO][Ag^+]$ of $5(\pm 2) \times 10^5$ was obtained by evaluating the amount of free silver ion in solution after filtering; that is, the solution is highly depleted from the silver ions.

Radiolytic Reduction of Silver Ions in a SiO_2 Matrix. The colloidal silver within the silica support was produced by irradiation. In the range of ionizing radiation used (up to a dose of 5 kGy), exposure to ionizing radiation of the silica causes no noticeable damage to the structure or its stability.

TEM measurements were performed on the composite materials irradiated at different dose rates and at a dose sufficient to reduce all silver ions (5kGy). In Figure 2a, the TEM image of silver sample in Sil4 irradiated at a high dose rate is shown. For comparison, Figure 2b shows the TEM image obtained for the same amount of silver reduced by irradiation at a lower dose rate. The influence of the reduction rate becomes obvious from simple image inspection. In both cases, the pores of the silica matrix are uniform in size in the whole volume of the solid. Silver particles of spherical shape dispersed in the amorphous silica could be detected. All the particles are well-separated from each other. Nevertheless, while they are homogeneously randomly distributed with a diameter of 2 nm in the mesoporous silica matrix irradiated at a high dose rate (7 MGy·h^{-1}), larger particles 3−4 nm in diameter and less homogeneously dispersed are observed when prepared at a lower dose rate (2.7 kGy·h^{-1}). Similar observations have been obtained for experiments in Sil2 (not shown, diameter of 1 nm at 7 MGy·h^{-1} and 1.6 nm at 2.7 kGy·h^{-1}) instead of Sil4. A dose rate effect on the formation of the silver particles apparently exist; a possible mechanism of formation is discussed below.

Figure 3 shows the absorption isotherms for the pure and as-prepared samples after completion of the reduction (5 kGy). In the case of Sil2, the adsorption−desorption isotherms exhibit a steep slop at low relative pressure and are of type I. The isotherm of Sil2BRIJ78 is usually characterized by a small hysteresis and by 3-nm pores associated with micropores (d < 2 nm).[19] The difference between our samples and those published recently is explained by the higher temperature of calcination.[18] Indeed, with increasing temperature, it was evidenced that the pore size decreases and that the specific surface area is lowered due to partial sample contraction. The isotherms for the silver-containing samples were similar in shape to the parent sample but with a lower total adsorption capacity (Figure 3). For the silver−silica samples, a BET surface area and a total pore volume smaller than that obtained for the reference were calculated. This results from the loading

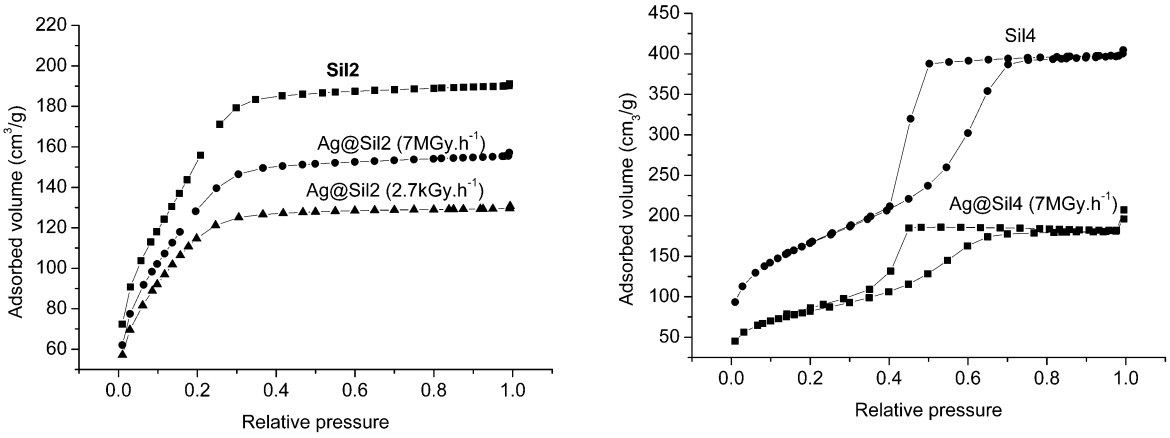

Figure 3. Nitrogen sorption isotherm before and after formation of silver particles in Sil2 (left) and Sil4 (right) after irradiation at different dose rate: 7.0 MGy·h^{-1} and 2.7 kGy·h^{-1}; dose = 5 kGy.

Table 1. Data Derived from Sorption and TEM Analysis of Samples

	surface area (m^2/g)	pore volume (cm^3/g)	size (TEM) (nm)
Sil2	580	0.28	
Ag@Sil2 (7 MGy·h^{-1})	490	0.20	1
Ag@Sil2 (2.7 kGy·h^{-1})	430	0.13	1.6
Sil4	600	0.60	
Ag@Sil4 (7 MGy·h^{-1})	300	0.34	2

of Ag metal onto the mesoporous silica materials, which restricts the amount of nitrogen adsorbed. Table 1 gives all the parameters calculated from the sorption data for the as-prepared silica samples.

A comparison of the adsorption data for the samples subjected to different irradiation dose rates, that is, reduction rates, reveals that the amount of nitrogen adsorbed and hence the effective surface area decreases when particles are produced with γ-radiolysis (2.7 kGy·h^{-1}) versus pulse irradiation (7 MGy·h^{-1}). This is obviously due to the fact that the silver nanoparticles have grown as large as the pores and thereby block larger parts of the pore system for the nitrogen molecules.

Experiments in the presence of Sil4 instead of Sil2 were conducted under the same irradiation conditions. Adsorption data on Sil4 silica, pure and with silver particles, have been reported in Table 1 and Figure 3b. For the Sil4 parent sample, the isotherm of nitrogen adsorption exhibit a steep slop at low relative pressure, indicating that it is not strictly of type IV. The isotherm is a superposition of types I and IV but with a large hysteresis loop between $P/P_0 = 0.2-0.4$, indicating the presence of micropores (diameter < 2 nm) and pores larger than the pore connections. This phenomenon was explained in detail earlier.[21] The micropores are related to the water- and silica-compatible PEO block which forms molecular pores of the size of a hydrated PEO chain diameter. A total pore volume for the Sil4 parent silica of 0.6 cm^3·g^{-1}, which therefore exhibits a higher overall porosity than Sil2. Similarly to the Sil2 samples, it was found that the presence of silver particles restricts the amount of nitrogen adsorbed, as indicated by smaller BET surface areas and pores volumes. Also in this case, the reduced apparent porosity can only be explained by a partial blocking of the mesopore system. In both cases, considering that all pores are occupied, we found that pores are not completely filled or blocked by silver nanoparticles (in volume) and are occupied by one particle. This corresponds to an unparalled spatial density of independent silver nanoparticles, as compared with the free solution case or traditional statistical deposits onto absorbing materials.

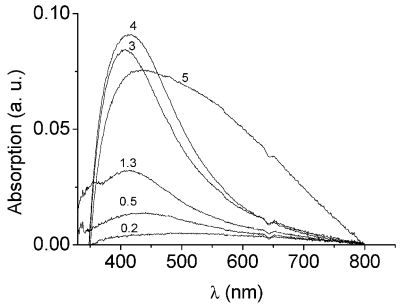

Figure 4. Evolution with increasing dose of the absorption spectra of a Sil4 silica containing silver ion irradiated at 2.7 kGy·h^{-1} by γ-rays: [Ag^I] = 10^{-2} mol·L^{-1}, pH = 7; doses (a−f) range from 0.5, 1.3, 3, 4, to 5 kGy.

To understand the formation process of the silver particles in the silica framework, samples were exposed to various radiation doses, and the optical spectrum of the generated particles was studied. The visible diffusing reflectance spectra for the silver−silica samples prepared at different γ-ray doses are shown in Figure 4. The pure silica shows very little absorption in this range. The Ag−silica samples irradiated with doses of up to 4 kGy display a plasmon resonance absorption centered at about 420 nm. This resonance is typical for isolated silver nanoparticles and shows that there is no electronic cross-talk between the single nanoparticles, although the particle density in the mesoporous support is extremely high. It is known from the literature that the intensity and the shape of these plasmon resonances depend on the dielectric environment surrounding the particle. In silicas, the plasmon resonance maximum of silver particles is often observed in the 400−440-nm region,[7−9] in good agreement with our own data (Figure 4).

The time dependence of the spectra (γ-irradiated for various lengths of time) show that already reduction of a very small amount of silver(I) leads to the development of the absorption band at around 420 nm. The

(21) Göltner, C. G.; Smarsly, B.; Berton, B.; Antonietti, M. *Chem. Mater.* **2001**, *13*, 1617.

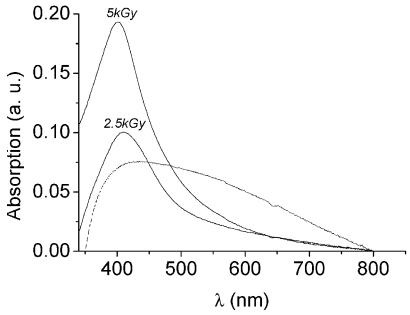

Figure 5. Evolution with increasing dose of the absorption spectra of a Sil4 silica containing silver ion irradiated at 7 MGy·h^{-1}: [Ag^{I}] = 10^{-2} mol·L^{-1}, pH = 7, dose = 2.5, and 5 kGy; (dotted line) spectrum obtained after irradiation with a γ-source (2.7 kGy·h^{-1}) and a dose of 5 kGy.

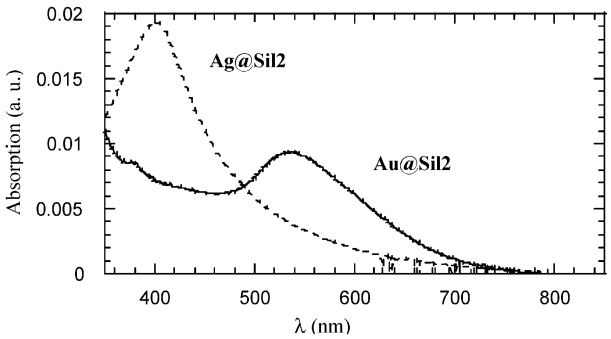

Figure 6. Evolution with time of the absorption spectra of a Ag@Sil2 silica exposed to solution containing gold ion: [$AuCl_4^-$] = 10^{-2} mol·L^{-1}; time difference between first and final spectrum is about 3 days.

peak becomes more pronounced as the irradiation becomes longer and the initially transparent silica turns light yellow. This corresponds essentially to an increase of the nanoparticle number, that is, nucleation and growth of the species are essentially going on throughout the process.

On further irradiation and reaching of doses of 5 kGy, the width of the surface plasmon resonance of silver particles markedly increases and the peak positions redshift. Here, the composite sample turns also macroscopically from yellow to dark gray. Both the massive shift to longer wavelength in the absorption spectra and the broadening of the resonance reflect the beginning electronic cross-talk of the particles or—correspondingly—a large size distribution of particles. Graphically spoken, the system starts to develop an extended metallic structure within the pore system. Those polydispersity and aggregation effects were confirmed from electron microscope observations. Similar effects and changes in the optical absorption spectra were observed upon the formation of silver particles during thermal reduction processes; the plasmon band of silver shifted gradually to higher wavelength as thermal annealing increased.[10]

For the targeted applications, it is therefore important to restrict the nanoparticle loading to the region where they are still well-separated.

In another set of experiments, silver−silica samples have been prepared under the same experimental conditions as in Figure 4 but at a much higher dose rate. Irradiation experiments have been performed with a pulsed electron beam facility delivering a dose rate of 7 MGy·h^{-1}. UV−vis spectra of the sample were measured. The spectra of the dose effect on the radiolysis of the silver−silica sample at 7 MGy·h^{-1} are shown in Figure 5.

When the silver−silica samples are irradiated at a rate at which the dose is delivered more rapidly, the intensity also increases with the dose, but all spectra present the same resonance band centered at 420 nm. The plasmon band shifts to higher wavelength and the transition is not found anymore in the applied range of silver concentrations and doses. For comparison, the spectrum of an identical but γ-irradiated sample (2.7 kGy·h^{-1}) with an overall dose of 5 kGy is also shown in Figure 5. With increasing dose rate, the resonance plasmon band is increased in intensity and narrowed. The sample obtained at a high dose rate remains yellow, which indicates the presence of a large number of isolated particles, whereas the other contains agglomerated particles.

This difference also gives important mechanistic information. With the pulse electron beam a dose of 5 kGy is delivered in a couple of seconds, as compared to over an almost 2-h time period under γ-irradiation conditions. At this dose, almost all the Ag^+ ions are transformed into silver atoms. As rapid reduction and the related high supersaturation always leads to higher nucleation rates and smaller particles (note that nucleation has a very high reaction order and therefore sensitively depends on species concentration), it is the better dispersion of the silver nanoparticles and presumably their better binding to the pore walls which gives the system made by pulsed electrons the better performance. The formation of small size isolated particles is in accordance with sorption analysis, indicating a lower volume loss with no micropores blocked, in contrast to the samples made by γ-irradiation. The influence of reduction rate on particle size also follows the general trends found for nanoparticle synthesis by chemical reduction methods.[22]

It has to be noted that, with respect to the colloidal stability of the samples, it is a general observation that the silver−silica samples kept their color and were stable for months without any sign of oxidation, illustrating the stabilizing role of the supporting mesoporous silica.

Au−Ag Exchange. The accessibility of the silver particles from the outside by analysts and reactants as well as the possibility to modify their structure was tested by a simple exchange experiment. Addition of the silver−silica sample irradiated at a high dose rate to a solution containing 10^{-3} mol·L^{-1} gold ions $AuCl_4^-$ lead to the disappearance of the silver absorption band and the formation of the absorption of gold particles (Figure 6). The silica, initially yellow, becomes pink-red within a couple of days. These observations imply that the gold ions diffuse through the "channels" into the pores where oxidation of silver particles takes place. This clearly demonstrates that the porosity of the silica matrix allows access of ionic reactant through the solid and that the silver nanoparticles have a redox potential lower than −1.5 V_{ENH} (far from that of the bulk material), allowing the formation of gold particles.[23]

Mechanism of Particles Formation. The mechanism of silver nanoparticles formation at the surface of

(22) Mayer, A.; Antonietti, M. *Colloid Polym. Sci.* **1998**, *276*, 769.

silica materials or in mesoporous materials has already been investigated by various authors.[24−29] The optical absorption band at 420 nm corresponds to the stable, relatively small, well-established colloidal silver particles. The silver particles formed have a redox potential lower than $-1.5\ V_{ENH}$. If we consider that the silica concentration is 200 mg·L^{-1} and that the cavity volume contains a concentration of 2 mol·L^{-1} of Ag^+, a radiolytic yield of 25 species per 100 eV was calculated. This is significantly higher than the value of the radiolytic yield in bulk solution, that is, $G = 6$ species/100 eV. This may be a consequence of the presence of other pathways for the reduction of Ag^+ than the formation of silver via the radiolytic species from aqueous solution. The strong coupling of Ag^+ to the silica structure presumably allows scavenging of additional electrons produced in the silica matrix. As already pointed out by Schatz et al., upon irradiation of aqueous solutions containing high-loading solid silica, the radiation energy is partially absorbed both by the aqueous solution and the mesoporous solid. Charge carriers produced in the silica cross the solid/liquid interface and the electron appears in the aqueous phase, whereas the holes remains trapped in the matrix:[30]

$$SiO_2 \xrightarrow{\gamma} e_{SiO_2}^- + h_{SiO_2}^+ \quad (6)$$

Consequently, the escaped electrons are involved in the reduction process of the silver ions. The silver metal ions attached to the solid surface (Ag_{ads}^+) or in the mesopore are reduced by the radiolytic species from the silica and the bulk aqueous phase located in the silica channels and the silica, according to reactions (7)−(9).

$$e^-_{(SiO_2)} + Ag_{ads}^+ \rightarrow Ag_{ads}^0 \quad (7)$$

$$e^-_s + Ag_{ads}^+ \rightarrow Ag_{ads}^0 \quad (8)$$

$$(CH_3)_2C^{\bullet}OH + Ag^+ \rightarrow Ag^0 + (CH_3)_2CO + H^+ \quad (9)$$

The hydrated electrons produced in the aqueous phase diffuse to the pore wall of the solid and along its surface to encounter an absorbed silver ion. A charge transfer from the hydrated electron to silica is unlikely because of the wide band gap of the insulating SiO_2.

Then, association reactions between adsorbed atoms Ag_{ads}^0 and excess Ag^+ ions rapidly occur at the surface as observed in free water:

$$Ag^0_{ads} + Ag^+ \rightarrow Ag_2^+{}_{ads} \quad \text{(association)} \quad (10)$$

$$Ag_2^+{}_{ads} + Ag^+ \rightarrow Ag_3^{2+}{}_{ads} \quad (11)$$

Scheme 1[a]

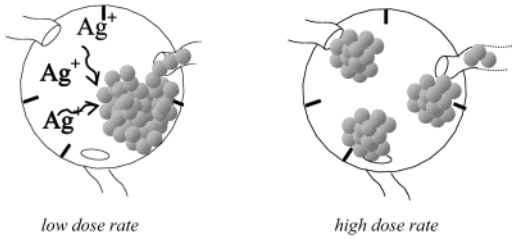

[a] Mechanism of formation of silver nanoparticles in the mesoporous silica (left) at a low dose rate and (right) at a high dose rate.

Since the concentration of these ions is fairly high in the mesoporous volume (2 mol·L^{-1}), it favors the formation of cationic silver particles $Ag_2^+{}_{ads}$ and $Ag_3^{2+}{}_{ads}$. Those species are strongly stabilized on the SiO_2 surface: they remain on both the anionic and the OH sites of the silica surface and do not desorb easily as already reported elsewhere.[30]

Reaction of those species with further silver ions or reduced atoms would result in the progressive building of particles of increasing size. When the nanoparticle size exceeds the size of a silver plasmon, it is characterized by the absorption at 400−440 nm.

One limiting process which determines the degree of agglomeration (the width of the size distribution) is the migration of the nanoparticles on the surface or through the silica channels. As revealed by the experiments with high dose rate, this overall diffusion of silver species along the surface and the mesochannels is obviously highly reduced, so the reaction is essentially carried via the very small ion and neutral silver clusters. In contrast, under conditions of low dose rate, only a few silver nuclei per unit volume are produced and grow by adsorption of the excess mobile free ions and species. The adsorbed ions are progressively reduced in situ on the surface of these nuclei upon increasing irradiation. This causes the growth of clusters of increasing size, presumably both in the micro- and mesopores, until they block the pores or contact each other. Such an agglomeration process within the overall matrix is also found when metal ions are progressively reduced by thermal treatment in which the reduction is in the range of hours.[6]

This is the reason for the superiority of the silver clusters made by electron beam radiation: they are more likely well-separated from each other and are homogeneously distributed (Scheme 1).

Conclusion

A very high density of well-defined, well-separated silver nanoparticles has been successfully incorporated into mesoporous silica via a radiolytic reduction of silver ions. The reduction of the silver in the matrix induced by radiation has been studied by optical absorption spectroscopy, electronic microscopy, and sorption measurements. The use of the radiation-induced synthesis allowed us to control the reduction rate through the dose conditions and thus to demonstrate its influence on the formation and the aggregation of the metal atoms. Metal reduction through the use of pulse installation at a very high dose rate yields silver nanoparticles of better homodispersity and markedly smaller size and limits the coalescence phenomena. It is expected that this

(23) Mosseri, S.; Henglein, A.; Janka, E. *J. Phys. Chem.* **1989**, *93*, 6791.
(24) Lawlees, D.; Kapoor, S.; Kennepohl, P.; Meisel, D.; Serpone, N. *J. Phys. Chem.* **1994**, *98*, 9619.
(25) Stein, A.; Ozin, G.A.; Stucky, G. D. *J. Soc. Photogr. Sci. Technol. Jpn.* **1990**, *53*, 322.
(26) Ozin, G. A. *Symp. Faraday Soc.* **1980**, *14*, 7.
(27) Ozin, G. A.; Hugues, F. *J. Phys. Chem.* **1983**, *87*, 94.
(28) Kellerman, R.; Texter, J. *J. Chem. Phys.* **1979**, *70*, 1562.
(29) Gachard, E.; Belloni, J.; Subramanian, M. A. *J. Mater. Chem.* **1996**, *6* (5), 867.
(30) Schatz, T.; Cook, A. R.; Meisel, D. *J. Phys. Chem. B* **1999**, *103*, 10209.

method can be extended to a general preparation technique for metallic nanoparticles in a wide range of concentration, always producing stable dispersions.

Furthermore, the control of the formation of metallic particles in the silica matrix also allows synthesis of composite particles with special optical properties such as luminescence. Especially promising is the case where, after their formation in situ, the metal−silica samples are mixed with a solution containing a luminescent center (M'^{+}), and a stable composite M_n/M'^{+} is formed. In order to synthesize Ag_n-Ag^{+} composite particles, only a partial reduction has to be achieved for composite formation in the silica framework. For this system, emission spectroscopy studies are currently underway and will be the subject of a forthcoming contribution.

Acknowledgment. The authors are gratefully indebted to the Max Planck Society and the French Minister of Education for financial support and to the University of Bordeaux II for having given us access to the γ-irradiation facility.

CM021353V